JOURNAL OF SOLID STATE CHEMISTRY 83, 52–60 (1989)

Oxidation–Reduction Behavior of Undoped and Sr-Doped $LaMnO_3$ Nonstoichiometry and Defect Structure

J. H. KUO AND H. U. ANDERSON

Ceramic Engineering Department, University of Missouri-Rolla, Rolla, Missouri 65401

AND D. M. SPARLIN

Physics Department, University of Missouri-Rolla, Rolla, Missouri 65401

Received March 7, 1989; in revised form July 3, 1989

Undoped and Sr-doped $LaMnO_3$ showed reversible oxidation–reduction behavior. These perovskites can be excess, stoichiometric or deficient in oxygen content depending on the specific conditions. Under very reducing conditions decomposition into new phases occurs. Phase stabilities for these oxides were determined. The results showed that Sr doping caused the $LaMnO_3$ to dissociate at higher oxygen activities than those necessary for undoped $LaMnO_3$. Defect models are proposed to interpret the thermogravimetric results in which metal vacancies are assumed for the oxygen excess condition and oxygen vacancies are assumed for the oxygen deficient condition. Thermodynamic properties were calculated which support the model. © 1989 Academic Press, Inc.

I. Introduction

The perovskite-type oxide $LaMnO_3$ has been extensively studied due to its potential application as an air electrode in high-temperature solid oxide fuel cells. The stability of the electrodes toward their environment is as important as their electrical conductivity for this application. Although several studies (*1–4*) on the oxidation reduction behavior of $LaMnO_3$ have been reported, a model relating the defect structure and the oxidation–reduction behavior of $LaMnO_3$ has never been proposed.

The objective of this study was to determine the phase stability and oxygen stoichiometry for undoped and Sr-doped $LaMnO_3$ as a function of oxygen partial pressure, temperature, and dopant concentration. In addition, a model was developed to explain the observed results.

II. Experimental Procedure

The undoped and Sr-doped $LaMnO_3$ specimens were prepared by a liquid mix method similar to that first described by Pechini (*5*). The starting chemicals were reagent grade La carbonate, Mn carbonate, and Sr carbonate. The desired compositions were prepared by dissolving quantitative amounts of selected carbonates into solutions of citric acid, ethylene glycol, and water. Upon removal of the excess solvent by heating, transparent solid resins containing the metals in solid solution were formed. Calcination of the resin intermediates at 800°C for 8 hr removed the organic

0022-4596/89 $3.00

constituents, leaving the desired ceramic compositions in a fine, uniform, and chemically combined state. For all compositions, X-ray diffraction analysis showed only the perovskite structure. No extra lines were detected.

Changes in stoichiometry at elevated temperatures were studied through thermogravimetry (TG) by measuring the weight change of a sample as a function of temperature and oxygen activity. Thirty to forty grams of powder samples were placed in a cylindrical alumina crucible and suspended from the balance by an alumina rod leading into a vertical tube furnace which was sealed from the atmosphere. The weight changes were measured to an accuracy of ± 1 mg. The desired furnace temperature was maintained to ± 2°C. Atmospheric control was achieved by using flowing gas mixtures (linear flow rate = 0.5 cm/sec) composed of either O_2–N_2 or CO_2-forming gas (10% H_2–90% N_2). A stabilized zirconia oxygen sensor was used to monitor the oxygen activity of the gas mixture. Thermogravimetric experiments were begun by fully oxidizing the sample in flowing oxygen until the equilibrium state was reached. The relative weight change was then measured as the oxygen activity, P_{O_2}, was reduced in a stepwise fashion. When the achievable P_{O_2} range had been covered, the sample was again reoxidized to its original state in order to determine if the process was reversible. Note that it is important to verify that reversibility occurs, since the defect structure analysis proposed in this study is based on the assumption that only one component of the compound is volatile. Significant errors may arise if irreversibility occurs.

In order to determine the phase change upon oxidation–reduction, X-ray diffraction patterns were made on undoped and Sr-doped $LaMnO_3$ samples which had been quenched from either oxidizing or reducing atmospheres. A sample for a quenching experiment was placed in an alumina tray and was transferred into an atmosphere-controlled multizone furnace. The hot zone was maintained at 1200°C while the cold zone was at 70°C. Oxidized samples were prepared by heating these powder samples in the hot zone with a flowing O_2 atmosphere for 2 days; they were then quenched by being rapidly pulled to the cold zone. The reduced samples were also quenched from 1200°C after annealing in flowing forming gas for 2 days.

III. Results and Discussion

A. Sr-Doped $LaMnO_3$

For Sr-doped $LaMnO_3$, the oxidized samples exhibited single phase X-ray patterns while the reduced samples were multiphase. The X-ray diffraction analysis showed that under the most reducing conditions (1200°C, 10^{-16} atm) Sr-doped $LaMnO_3$ completely dissociated into La_2O_3, MnO, $SrMnO_3$, and La_2MnO_4. Upon reoxidation, the reduced samples regained their original single-phase X-ray patterns indicating that the redox cycle is reversible.

In order to carry out the defect structure analysis, experimental TG data (weight loss vs log P_{O_2}) must be converted into molar oxygen content vs log P_{O_2}. Therefore a reference state is required. The reference state of molar oxygen content is often chosen at either the most oxidative or the most reducing condition if the molar oxygen content under either condition is a known stoichiometric value. For Sr-doped $LaMnO_3$, the molar oxygen content under the oxidative condition is unknown, while under reducing conditions one of the dissociated phases, $SrMnO_3$, is nonstoichiometric (6). Therefore, neither the oxidative nor the reducing condition can serve as a reference state. However, similar to the study of the $La_{1-x}Sr_xFeO_3$ system by Mizusaki *et al.* (7), the conversion of weight loss to molar oxy-

gen content for Sr-doped $LaMnO_3$ was achieved by using Wagner's statistical thermodynamic theory (*8*). This was done by assuming the flat region observed in weight loss vs log P_{O_2} data to be the stoichiometric state of the oxide. By using the stoichiometric state as the reference point, the weight loss was then converted to molar oxygen content. Defect structures were proposed to interpret the thermogravimetric results in which metal vacancies and oxygen vacancies were assumed for the oxygen excess condition and oxygen deficient condition, respectively. These regions are discussed below.

1. Oxygen excess region ($La_{1-y}Sr_yMnO_{3+x}$). According to the X-ray diffraction data of Wollan and Koehler (*9*), $LaMnO_3$ preparations are characterized by cation vacancies rather than by interstitial anions. Tofield and Scott (*10*) reported from neutron diffraction analysis that the structure for $LaMnO_{3.12}$ contained vacancies on both La and Mn sites. It is therefore assumed that in the high P_{O_2} region, metal vacancies on both La and Mn sites are the predominant defects. For simplicity, the metal vacancies are assumed to be fully ionized at the high temperatures. Furthermore, it is assumed that charge conservation related with Sr incorporation is obtained on Mn lattice sites.

Using Kroger–Vink notation (*11*), in the oxygen excess region the reduction of $La_{1-y}Sr_yMnO_{3+x}$ may be expressed as

$$La_{1-y}Sr'_yV'''_{La_{x/3}}Mn^x_{1-y-2x}Mn^{\cdot}_{y+2x}V'''_{Mn_{x/3}}O_{3+x} \rightleftarrows La_{1-y}Sr'_yMn^x_{1-y}Mn^{\cdot}_yO_3 + x/2\ O_2, \quad (1)$$

where y represents the dopant and x the excess oxygen concentration. In terms of reactants this reaction can be simplified to

$$V'''_{La} + V'''_{Mn} + 6Mn^{\cdot}_{Mn} + 3O_0 \rightleftarrows 6Mn^x_{Mn} + \tfrac{3}{2}\ O_2 \quad (2)$$

If it is further assumed that if $[V'''_{La}] = [V'''_{Mn}]$, then the equilibrium constant for this reaction is given by

$$K_2 = [Mn^x_{Mn}]^6\ P^{3/2}_{O_2}/\{[V'''_{La}]^2\ [Mn^{\cdot}_{Mn}]^6\ [O_0]^3\}, \quad (3)$$

which in terms of mole fraction becomes

$$K_2 = (1 - y - 2x)^6\ P^{3/2}_{O_2}/\{(x/3)^2\ (y + 2x)^6\ (3 + x)^3\}. \quad (4)$$

For a given dopant level y, K_2 can be found from the weight loss vs P_{O_2} experimental data by using Eq. (4). Theoretical curves in the high P_{O_2} region were generated by using K_2 and the proposed metal vacancy model.

2. Oxygen deficient region ($La_{1-y}Sr_yMnO_{3-x}$). On the basis of the assumptions that $LaMnO_3$ has *p*-type nonstoichiometric disorder, (*12*), that a stoichiometric La/Mn ratio is maintained (*13*), that $LaMnO_3$ remains single phase, and that all of the defects are fully ionized, the reduction of Sr-doped $LaMnO_3$ in the low P_{O_2} regions can be represented by

$$La_{1-y}Sr^{\cdot}_yMn^x_{1-y}Mn^{\cdot}_yO_3 \rightleftarrows La_{1-y}Sr'_yMn^x_{1-y+2x}Mn^{\cdot}_{y-2x}V^{\cdot\cdot}_{0x}O_{3-x} + x/2\ O_2 \quad (5)$$

or

$$2Mn^{\cdot}_{Mn} + O_0 \rightleftarrows 2Mn^x_{Mn} + V^{\cdot\cdot}_0 + \tfrac{1}{2}\ O_2. \quad (6)$$

The equilibrium constant for Eq. (6) is given by

$$K_6 = [Mn^x_{Mn}]^2\ [V^{\cdot\cdot}_0]P^{1/2}_{O_2}/[Mn^{\cdot}_{Mn}]^2\ [O_0]. \quad (7)$$

Since at very low P_{O_2} part of the Mn ions are expected to be divalent, the general neutrality condition can be represented by

$$[Sr'_{La}] + [Mn'_{Mn}] = 2[V^{\cdot\cdot}_0] + [Mn^{\cdot}_{Mn}]. \quad (8)$$

The relation between $[Mn^{\cdot}_{Mn}]$ and $[Mn'_{Mn}]$ is given by

$$2Mn^x_{Mn} \rightleftarrows Mn'_{Mn} + Mn^{\cdot}_{Mn}, \quad (9)$$

with

$$K_9 = [Mn_{Mn}^{\cdot}][Mn_{Mn}^{\prime}]/[Mn_{Mn}^{x}]^2. \quad (10)$$

In order to maintain the fixed A/B ratio, the following equation must be maintained:

$$[Mn_{Mn}^{x}] + [Mn_{Mn}^{\cdot}] + [Mn_{Mn}^{\prime}] = 1. \quad (11)$$

By combining the experimental TG data with Eqs. (7), (8), (10), and (11), the equilibrium constants K_6 and K_9 can be calculated.

The theoretical isotherms for the P_{O_2} range investigated were generated from the calculated equilibrium constants, K_2, K_6 and K_9. The TG results for $La_{1-y}Sr_yMnO_3$ ($y = 0.01$, 0.1, and 0.2) are shown in Figs. 1 to 3, in which the symbols represent the experimental data while the lines were calculated. As can be seen in Figs. 1 to 3 the calculated isotherms fit the data quite well even in the regions for which the perovskite starts to dissociate into new phases. For each isotherm shown in Figs. 1 to 3, the symbol at the lowest P_{O_2} value indicates the "critical" point, i.e., the lowest P_{O_2} before the oxide dissociated into multiple phases.

B. Undoped $LaMnO_3$

X-ray analysis showed that upon reduction $LaMnO_3$ also dissociated into two phases identified as La_2O_3 and MnO. Since both La_2O_3 and MnO show negligible oxygen nonstoichiometry under highly reducing conditions (*14*), these two phases provide a reference state for the molar oxygen content which is equivalent to $LaMnO_{2.5}$. By using this reference point, the stoichiometric oxygen content of $LaMnO_3$ at 1000°C was determined to be 2.999. This result suggested that undoped $LaMnO_3$ might possess vacancies on the La lattice which are equivalent to an acceptor content of 0.2 mol%. Therefore, the analysis of TG data for undoped $LaMnO_3$ used the same set of equations described in the previous section. Both experimental data and calculated values are shown in Fig. 4.

The observed molar oxygen content for undoped $LaMnO_3$ at 1200°C ranged from 3.063 to 2.977. This result agrees well with a previous investigator (*1*), who found that at the same temperature the molar oxygen content ranged from 3.079 to 2.947. The

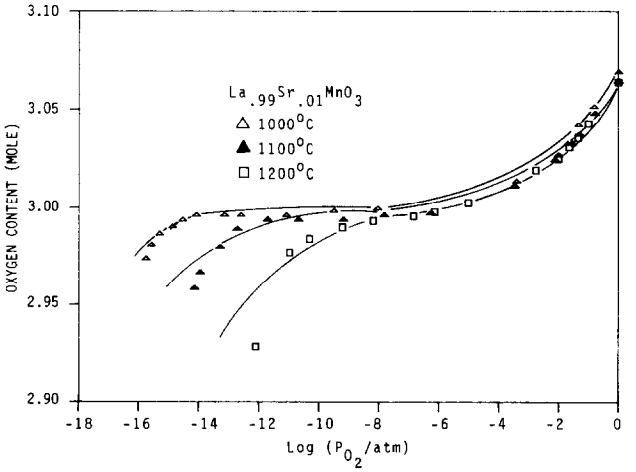

FIG. 1. Moles oxygen per mole $La_{.99}Sr_{.01}MnO_3$ vs log P_{O_2} at various temperatures. The solid lines are calculated. For each isotherm, the last point represents the lowest P_{O_2} before the oxide decomposed completely to multiple phases.

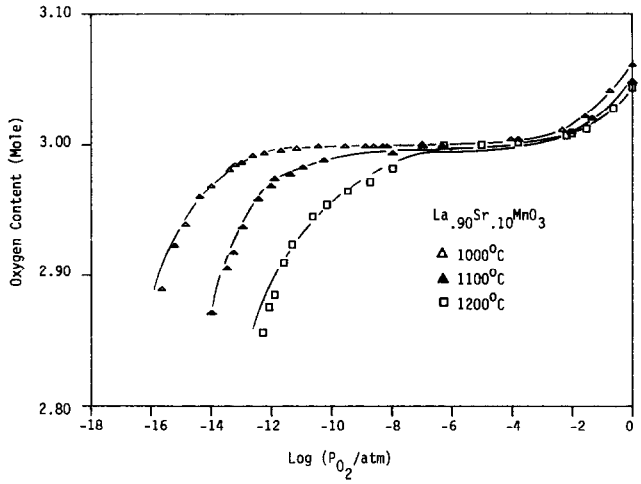

FIG. 2. Moles oxygen per mole $La_{.90}Sr_{.10}MnO_3$ vs log P_{O_2} at various temperatures. The solid lines are calculated. For each isotherm, the last point represents the lowest P_{O_2} before the oxide decomposed completely to multiple phases.

slight difference in the oxygen stoichiometry may have resulted from differences in sample preparation. The critical P_{O_2} values reported by different authors are compared in Table I. The discrepancies in the critical P_{O_2} values may be due to different experimental P_{O_2} control techniques and differences in the types of measurements as discussed elsewhere (*15–17*).

The behavior of Sr-doped $LaMnO_3$ equilibrated at 1000°C is shown in Fig. 5. The behavior of undoped and Sr-doped $LaMnO_3$ were similar. The following general characteristics were observed for all samples:

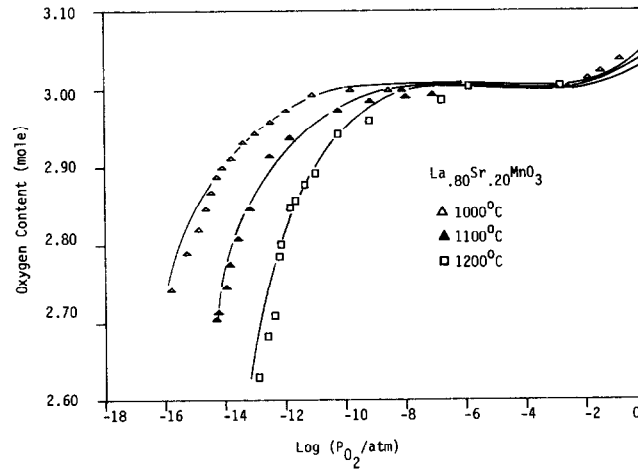

FIG. 3. Moles oxygen per mole $La_{.80}Sr_{.20}MnO_3$ vs log P_{O_2} at various temperatures. The solid lines are calculated. For each isotherm, the last point represents the lowest P_{O_2} before the oxide decomposed completely to multiple phases.

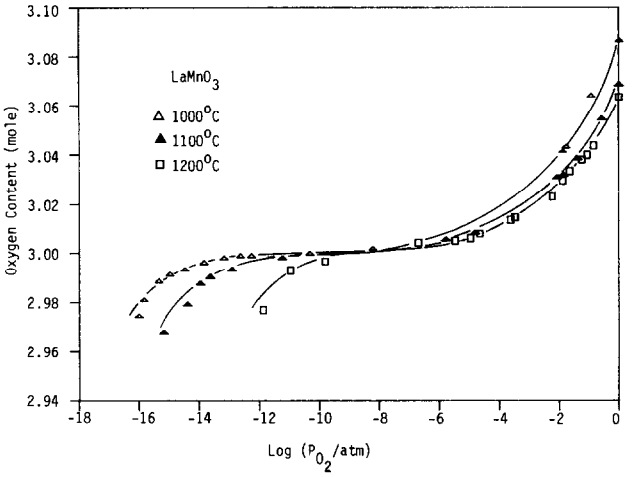

FIG. 4. Moles oxygen per mole $LaMnO_3$ vs log P_{O_2} at various temperatures. The solid lines are calculated. For each isotherm, the last point represents the lowest P_{O_2} before the oxide decomposed completely to multiple phases.

(i) All of the oxides exhibited three distinct regions which were oxygen excess, stoichiometric, and oxygen deficient.

(ii) Under very reducing conditions, decomposition into new phases occurred at a "critical" P_{O_2}. These values shifted to higher P_{O_2} with increasing temperature.

(iii) The amount of excess oxygen decreased with increasing temperature.

The effects of Sr addition on the oxidation–reduction behavior showed common trends with increasing dopant content:

(i) The amount of excess oxygen decreased.

(ii) The critical P_{O_2} was shifted to higher P_{O_2}.

C. Thermodynamic Considerations of the Defect Models

1. Oxygen excess region (metal vacancy model). The equilibrium constants for metal vacancy formation in the oxygen excess region, K_2, are listed in Table II. By using these equilibrium constants, the relationship between molar oxygen excess (x) and partial oxygen activity (P_{O_2}) can be calculated. Some useful thermodynamic quan-

TABLE I

CRITICAL LOG P_{O_2} FOR $LaMnO_3$ AT 1200°C

	Log (P_{O_2}/atm)	Type of measurement
Kamata (*1*)	−11.65	TGA
Kamagashira (*15*)	−11.64	Conductivity
Sreedharan (*16*)	−10.3[a]	EMF
This study	−11.9	TGA

[a] Estimated.

TABLE II

EQUILIBRIUM CONSTANTS, K_2, CALCULATED FROM OXYGEN EXCESS MODELS (EQ. (1))

	Log equilibrium constant, K_2		
Compound	1000°C	1100°C	1200°C
Undoped $LaMnO_3$	−5.66	−6.58	−6.92
$La_{.99}Sr_{.01}MnO_3$	−6.35	−6.63	−6.74
$La_{.95}Sr_{.05}MnO_3$	−5.75	−6.47	−7.27
$La_{.90}Sr_{.10}MnO_3$	−5.18	−5.84	−6.10
$La_{.80}Sr_{.20}MnO_3$	−4.25	−4.83	−4.97

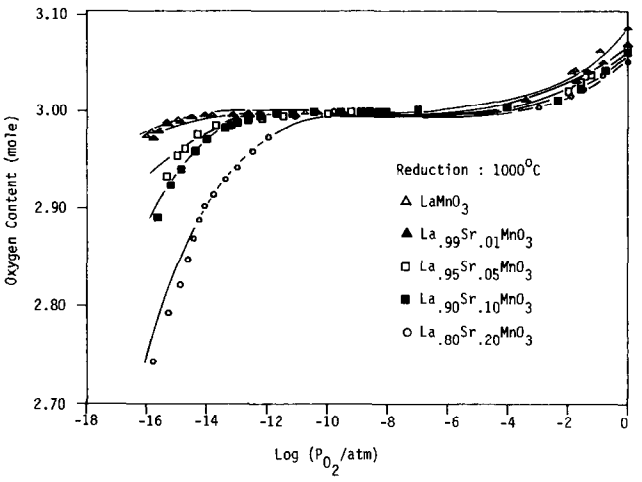

FIG. 5. Moles oxygen per mole sample vs log P_{O_2} for various Sr-dopant levels at 1000°C. The solid lines are calculated. For each isotherm, the last point represents the lowest P_{O_2} before the oxide decomposed completely to multiple phases.

tities such as $\Delta\bar{G}_{O_2}$, the relative partial molar free energy of oxygen, $\Delta\bar{S}_{O_2}$, the relative partial molar entropy of oxygen, and $\Delta\bar{H}_{O_2}$, the partial molar enthalpy of oxygen, can be easily calculated according to the following equations:

$$\Delta\bar{G}_{O_2} = RT \ln P_{O_2}, \tag{12}$$

$$\Delta\bar{S}_{O_2} = -\delta(\Delta\bar{G}_{O_2})/\delta T, \tag{13}$$

and

$$\Delta\bar{H}_{O_2} = \Delta\bar{G}_{O_2} + T\Delta\bar{S}_{O_2}. \tag{14}$$

The calculated partial molar free energies for undoped $LaMnO_{3+x}$ are shown in Fig. 6. These partial molar free energies were found to be a function of temperature and molar oxygen excess. The bivariant behavior indicates that the oxygen excess region

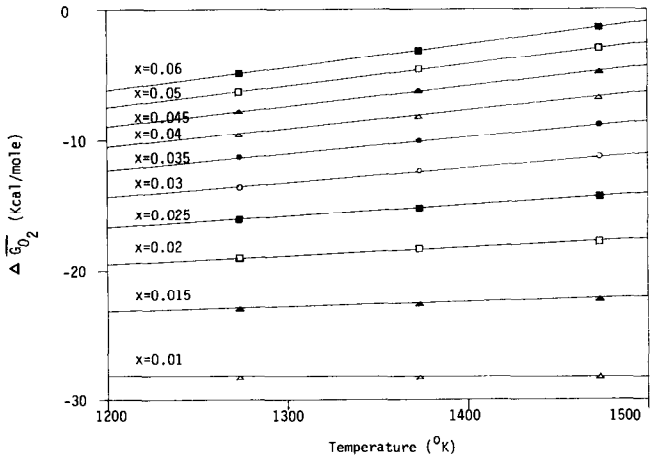

FIG. 6. Relative partial molar free energy for a solution of diatomic oxygen in $LaMnO_3$ phase as a function of temperature. The solid lines are calculated by means of a least-squares analysis.

($LaMnO_{3+x}$) can be considered as a single phase across its composition (x) range (*18*). The results for Sr-doped $LaMnO_{3+x}$ are not shown since they are similar to those of undoped $LaMnO_{3+x}$. The effects of Sr dopant concentration on the relative partial molar entropy are shown in Fig. 7. It was found that $\Delta\bar{S}_{O_2}$ decreases with increasing molar oxygen excess (x). This qualitatively agrees with the previous results of Kamegashira (*4*). However, the slope of the $\Delta\bar{S}_{O_2}$ vs x plot observed in this study is larger than that by Kamegashira. The calculated values for $\Delta\bar{S}_{O_2}$ for all of the oxides investigated were negative. This has significance since $\Delta\bar{S}_{O_2}$ is expected to be negative for nonstoichiometric oxides if a metal vacancy mechanism (*14*) occurs.

The relative partial enthalpies ($\Delta\bar{H}_{O_2}$) were calculated from Eq. (14). It was found that $\Delta\bar{H}_{O_2}$ is independent of the degree of oxygen excess (x). This result tends to agree with the assumption that metal vacancies prevail, since a value for $\Delta\bar{H}_{O_2}$ which is independent of x is expected for randomly distributed and noninteracting metal vacancies.

The results obtained for $\Delta\bar{H}_{O_2}$ as a function of dopant level are shown in Table III. As can be seen no dependence within experimental error on dopant concentration was observed.

TABLE III

RELATIVE PARTIAL MOLAR ENTHALPY FOR UNDOPED AND Sr-DOPED $LaMnO_3$

Compound	$\Delta\bar{H}_{O_2}$ (kJ/mole)
Undoped $LaMnO_3$	-114.5 ± 13
$La_{.99}Sr_{.01}MnO_3$	-115.8 ± 13
$La_{.95}Sr_{.05}MnO_3$	-114.5 ± 13
$La_{.90}Sr_{.10}MnO_3$	-114.5 ± 13
$La_{.80}Sr_{.20}MnO_3$	-115.8 ± 13

Another set of thermodynamic properties $\Delta\bar{H}_{0x}$ and $\Delta\bar{S}_{0x}$, the standard enthalpy and entropy change for the formation of metal vacancies, can be found using the relationship

$$-RT \ln K_{0x} = \Delta\bar{H}_{0x} - T\Delta\bar{S}_{0x}. \quad (15)$$

For oxygen excess models the equilibrium constant, K_{0x}, is equivalent to K_2 for undoped $LaMnO_3$ and Sr-doped $LaMnO_3$. By substituting the equilibrium constants (Table II) into Eq. (15), $\Delta\bar{H}_{0x}$ and $\Delta\bar{S}_{0x}$ were calculated using a least-squares method. The results are shown in Table IV.

2. Oxygen deficient region. The region could not be treated as extensively as the

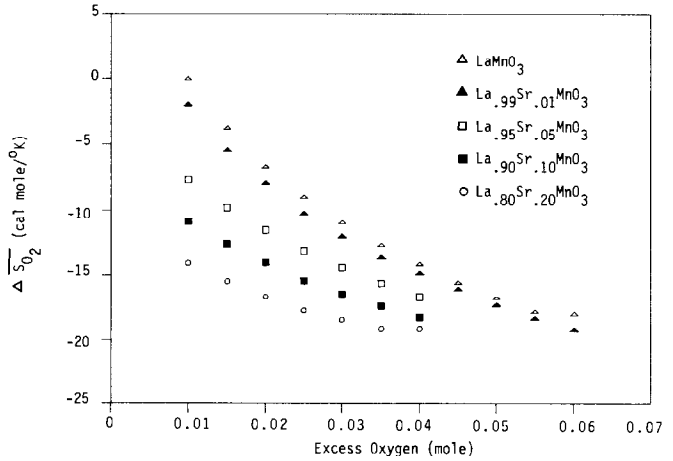

FIG. 7. Relative partial molar entropy of oxygen vs excess oxygen for various Sr-dopant levels.

TABLE IV

STANDARD ENTHALPY AND ENTROPY CHANGE FOR THE FORMATION OF METAL VACANCIES (EQ. (2))

Compound	$\Delta\bar{H}_{0\alpha}$ (kJ/mole)	$\Delta\bar{S}_{0\alpha}$ (J/mole °K)
Undoped $LaMnO_3$	631 ± 170	−234 ± 30
$La_{.99}Sr_{.01}MnO_3$	631 ± 170	−234 ± 30
$La_{.95}Sr_{.05}MnO_3$	627 ± 170	−226 ± 30
$La_{.90}Sr_{.10}MnO_3$	589 ± 170	−213 ± 30
$La_{.80}Sr_{.20}MnO_3$	564 ± 170	−188 ± 30

oxygen excess region because two competing reactions (Eq. (6) and Eq. (9)) coexisted. In addition, it was difficult to determine precisely where the oxides became multiple phase. Thus it was only possible to determine the enthalpy of formation of oxygen vacancies (Eq. (6)) and valency change of Mn (Eq. (9)). The temperature dependence of K_6 yielded a value of 360 ± 21 kJ/mole for the formation energy of oxygen vacancies. The constant K_9 gave values of 38 ± 8 kJ/mole and 84 ± 8 kJ/mole for the enthalpy change associated with the valency changes of Mn in Sr-doped $LaMnO_3$ and $LaMnO_3$, respectively. No data has been found with which to compare these results except that of Anderson *et al.* (*19*), in which they obtained a value of 272 ± 17 kJ/mole for the formation energy of oxygen vacancies in Mg-doped $LaCrO_3$.

IV. Conclusion

The undoped and Sr-doped $LaMnO_3$ specimens all showed three regions of oxygen stoichiometry: oxygen excess, oxygen deficient or stoichiometric. Under very reducing conditions these oxides decompose into new phases. The oxidation–reduction behavior was found to be reversible and the critical P_{O_2} values for decomposition were determined by TG measurements. The phase stability of $LaMnO_3$ against reduction was shifted to higher P_{O_2} when the temperature and/or Sr-dopant concentrations increased.

A metal vacancy model was adopted for the interpretation of the oxygen excess data while oxygen vacancies were assumed to be the predominant defect in the oxygen deficient region. Positive confirmation for the validity of the proposed defect models was achieved from thermodynamic considerations.

References

1. K. KAMATA, T. NAKAJIMA, T. HAYASHI, AND T. NAKAMURA, *Mater. Res. Bull.* **13,** 49 (1978).
2. T. NAKAMURA, G. PETZOW, AND L. J. GAUCKLER, *Mater. Res. Bull.* **14,** 649 (1979).
3. YU. P. VOROB'EV, A. A. NOVLEV, S. A. LEONT'EV, A. N. MEN, S. A. PROKUDINA, AND YA. S. RUBINCHIK, *Inorg. Mater.* **15,** 1142 (1979).
4. N. KAMEGASHIRA AND Y. MIYAZAKI, *Mater. Chem. Phys.* **11,** 187 (1984).
5. M. P. PECHINI, "Method of Preparing Lead and Alkaline Earth Titanates and Niobates and Coating Method Using the Same to Form a Capacitor," US Patent 3,330,697.
6. T. NEGAS AND R. ROTH, *J. Solid State Chem.* **1,** 409 (1970).
7. J. MIZUSAKI, M. YOSHIHIRO, S. YAMAUCHI, AND K. FUEKI, *J. Solid State Chem.* **58,** 257 (1985).
8. C. WAGNER, *Prog. Solid State Chem.* **6,** 1 (1971).
9. E. O. WOLLAN AND W. C. KOEHLER, *Phys. Rev.* **100,** 545 (1955).
10. B. C. TOFIELD AND W. R. SCOTT, *J. Solid State Chem.* **10,** 183 (1974).
11. F. A. KROGER, "The Chemistry of Imperfect Crystals," North-Holland, Amsterdam (1964).
12. J. H. KUO, "Studies of Defect Structure and Oxidation–Reduction Behavior of Undoped $LaMnO_3$, Sr-doped $LaMnO_3$ and Mg-doped $LaMnO_3$," Ph.D. thesis, University of Missouri-Rolla (1987).
13. F. ABBATTISTA AND M. LUCCO BORLERA, *Ceram. Int.* **7,** 137 (1981).
14. P. KOFSTAD, "Nonstoichiometry, Diffusion and Electrical Conductivity in Binary Metal Oxides," Wiley, New York (1972).
15. N. KAMEGASHIRA, Y. MIYAZAKI, AND Y. HIYOSHI, *Mater. Lett.* **2,** 194 (1984).
16. O. M. SREEDHARAN, R. PANKAJAVALLI, AND J. B. GNANAMOORTHY, *Mater. Lett.* **2,** 547 (1984).
17. N. KAMEGASHIRA, *Mater. Lett.* **2,** 549 (1984).
18. O. T. SORENSEN, "Nonstoichiometric Oxides," Academic Press, New York (1981).
19. H. U. ANDERSON, M. M. NASRALLAH, B. K. FLANDERMEYER, AND A. K. AGARWAL, *J. Solid State Chem.* **56,** 325 (1985).